



НАНОТЕХНОЛОГИИ, НАНОМАТЕРИАЛЫ И МЕТАМАТЕРИАЛЫ

Известия Саратовского университета. Новая серия. Серия: Физика. 2021. Т. 21, вып. 3. С. 285–292

Izvestiya of Saratov University. Physics, 2021, vol. 21, iss. 3, pp. 285–292

<https://fizika.sgu.ru>

<https://doi.org/10.18500/1817-3020-2021-21-3-285-292>

Article

Fluorescent nanostructures based on folic acid and citrate: Synthesis and properties

E. A. Mordovina , D. V. Tsyupka, A. A. Bakal,
A. M. Abramova, I. Yu. Goryacheva

Saratov State University, 83 Astrakhanskaya St., Saratov, 410012 Russia

Ekaterina A. Mordovina, mordovina_ekaterina@mail.ru, <https://orcid.org/0000-0003-1773-9015>

Daria V. Tsyupka, tsyupkadv@mail.ru, <https://orcid.org/0000-0002-4177-6257>

Artem A. Bakal, artembakal95@gmail.com, <https://orcid.org/0000-0002-3260-4744>

Anna M. Abramova, vostrikova2401@bk.ru, <https://orcid.org/0000-0003-0666-7685>

Irina Yu. Goryacheva, goryachevaiy@mail.ru, <https://orcid.org/0000-0003-1781-6180>

Abstract. The fluorescent properties of products obtained by the hydrothermal treatment of organic raw materials are of great interest. Such products are usually colloidal stability in water, have low cytotoxicity, and high photostability. One of their advantages is a wide choice of starting materials and the relative simplicity of synthesis. The use of folic acid as a precursor for fluorescent nanostructures opens up the possibility of targeted imaging. This article shows a one-step synthesis of fluorescent nanostructures from folic acid and citrates. The effect of citrate concentration in the range from 0.05 to 2 mol/l on the optical properties of the synthesized structures is also studied.

Keywords: fluorescent nanostructures, one-step synthesis, hydrothermal synthesis, folic acid, citric acid, sodium citrate, water-soluble nanostructures


Acknowledgements: The work was supported by the Ministry of Science and Higher Education of the Russian Federation (project No. FSRR-2020-0002).

For citation: Mordovina E. A., Tsyupka D. V., Bakal A. A., Abramova A. M., Goryacheva I. Yu. Fluorescent nanostructures based on folic acid and citrate: Synthesis and properties. *Izvestiya of Saratov University. Physics*, 2021, vol. 21, iss. 3, pp. 285–292 (in Russian). <https://doi.org/10.18500/1817-3020-2021-21-3-285-292>

This is an open access article distributed under the terms of Creative Commons Attribution 4.0 International License (CC-BY 4.0)

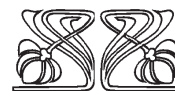
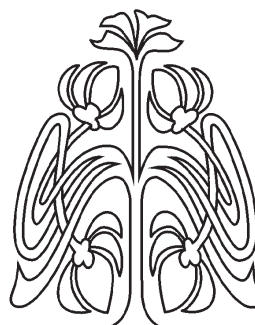
УДК 535.372

Флуоресцентные наноструктуры на основе фолиевой кислоты и цитратов: синтез и свойства

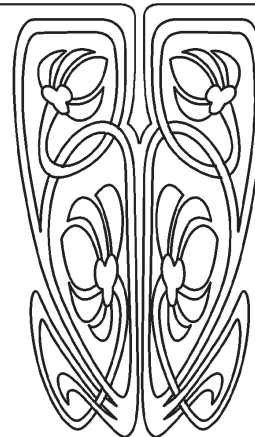
E. A. Mordovina , Д. В. Цюпка, А. А. Бакал,
А. М. Абрамова, И. Ю. Горячева

Саратовский национальный исследовательский государственный университет имени Н. Г. Чернышевского, Россия, 410012, г. Саратов, ул. Астраханская, д. 83

Мордовина Екатерина Алексеевна, магистр, сотрудник лаборатории дистанционно управляемых систем для тераностики, mordovina_ekaterina@mail.ru, <https://orcid.org/0000-0003-1773-9015>



НАУЧНЫЙ
ОТДЕЛ





Цюпка Дарья Владиславовна, магистр, сотрудник лаборатории неорганической химии, tsyupkadv@mail.ru, <https://orcid.org/0000-0002-4177-6257>

Бакал Артем Алексеевич, аспирант, сотрудник лаборатории неорганической химии, artembakal95@gmail.com, <https://orcid.org/0000-0002-3260-4744>

Абрамова Анна Михайловна, кандидат химических наук, доцент кафедры общей и неорганической химии, vostrikova2401@bk.ru, <https://orcid.org/0000-0003-0666-7685>

Горячева Ирина Юрьевна, доктор химических наук, профессор кафедры общей и неорганической химии, goryachevaiy@mail.ru, <https://orcid.org/0000-0003-1781-6180>

Аннотация. Флуоресцентные свойства материалов, получаемых гидротермальной обработкой органических молекул-прекурсоров, вызывают большой интерес. Такие наноструктуры обладают коллоидной стабильностью в воде, низкой цитотоксичностью и высокой фотостабильностью. Одно из их преимуществ – широкий выбор исходных материалов и относительная простота синтеза. Использование фолиевой кислоты в качестве прекурсора для флуоресцентных наноструктур открывает возможность направленной визуализации. В данной статье показана одноэтапная схема синтеза флуоресцентных наноструктур из фолиевой кислоты и цитратов, изучено влияние концентрации цитрата в диапазоне от 0.05 до 2 моль/л на оптические свойства синтезированных структур.

Ключевые слова: флуоресцентные наноструктуры, одностадийный синтез, гидротермальный синтез, фолиевая кислота, лимонная кислота, цитрат натрия, водорастворимые наноструктуры

Благодарности: Работа выполнена при финансовой поддержке Министерства науки и высшего образования Российской Федерации (проект № FSRR-2020-0002).

Для цитирования: Mordovina E. A., Tsyupka D. V., Bakal A. A., Abramova A. M., Goryacheva I. Yu. Fluorescent nanostructures based on folic acid and citrate: Synthesis and properties [Мордовина Е. А., Цюпка Д. В., Бакал А. А., Абрамова А. М., Горячева И. Ю. Флуоресцентные наноструктуры на основе фолиевой кислоты и цитратов: синтез и свойства] // Известия Саратовского университета. Новая серия. Серия: Физика. 2021. Т. 21, вып. 3. С. 285–292. <https://doi.org/10.18500/1817-3020-2021-21-3-285-292>

Статья опубликована на условиях лицензии Creative Commons Attribution 4.0 International (CC-BY 4.0)

Introduction

Folic acid (FA) is a member of the B vitamins, the pterin family. FA is involved in many biological processes. In this regard, the presence of FA in the body is vital. Cells metabolize FA using specific folate receptors. FA molecules interact with receptors through the pterin fragment [1]. It is known that the activity of folate receptors in cancer cells is significantly higher than in healthy cells [1,2]. This allows FA to be used as a targeting ligand for cancer cells. As a result of the functionalization of various carriers with FA, magnetic-resonance contrast agents [3,4], radiopharmaceutical imaging agents [5], chemotherapy protocols [6], rapid tests for FA detection [7], were developed. Obtaining such systems is usually a difficult task and usually includes the steps of modifying of carrier surface with folic acid [8] or preparing conjugates [7]. In this regard, new approaches to synthesis of FA-functionalized structures are needed.

Pterins exhibit intense fluorescence in the blue region of the spectrum, while the FA molecule has a low fluorescence quantum yield (QY). This is due to the fact that the substituent of glutamyl-p-aminobenzoic acid acts as an “internal quencher”, as evidenced by the values of the QY of various representatives of pterins (Table). At the pH range 3 to 13 most pterins can exist in several acid-base forms. The dominant equilibrium includes an am-

ide group (acid form) and a dissociated phenolic group (base form). At pH 4.9–5.5 and 10.0–10.5, pterins exist by more than 99% in acid and base forms, respectively. The QY value for the basic forms is lower than for the acidic ones (Table), this is due to the fact that at a pH above 11, the fluorescence of pterins is quenched by hydroxide ions [9].

Ultraviolet irradiation [10] or heat treatment [11,12] of FA solution can significantly increase its emission QY. Some articles describing the thermal treatment of FA have reported an increase in the QY due to its degradation or nanoparticle formation. However, the solo use of such a product as targeting and visualizing ligand remains difficult. This is due to the fact that the spectrum of FA fluorescence, as well as the products of its heat treatment, coincides with the autofluorescence of most of the cells.

Based on the studied literature, we assume that the structures obtained by us have nanometer dimensions. Therefore, we call the resulting product fluorescent nanostructures. In the future, we plan to study their size and morphology.

Thus, development of a simple synthesis of targeting systems with FA, having long-wavelength fluorescence is a challenging task. In this manuscript, we report synthesis and properties of fluorescent nanostructures (FNSs) via hydrothermal co-treatment of FA and other organic precursors.



Table. Fluorescence quantum yield of some pterins (λ_{ex} 350 nm; air)

Compound	Structure	Quantum yield acid (base) form [9]
Folic acid		<0.005 (<0.005)
6-carboxypterin		0.27 (0.20)
6-formylpterin		0.12 (0.07)
Pterin		0.32 (0.27)

1. Experimental section

1.1. Synthesis of fluorescent nanostructures

FNSs were obtained by hydrothermal co-treatment of FA and citric acid (CA); or FA and sodium citrate (CitNa). The CA and CitNa concentration ranged from 0.05 to 2 mol/l, while the FA concentration was constant (10^{-3} mol/l). CA was chosen because it has proven itself as a starting material for the production of highly fluorescent structures, which are obtained by co-treatment with various amines [13–15]. This is usually attributed to the presence of several carboxyl groups in its structure [13]. CA salts, in particular CitNa, are interesting, since carbonyl and dissociated carboxyl groups remain available in their structure, and CitNa solutions have an alkaline medium, which contributes to the complete dissolution of FA.

Briefly, a series of solutions containing 10^{-3} mol/l of FA was prepared, with additions of 0, 0.05, 0.1, 0.5, 1, 1.5, and 2 mol/l CA or CitNa (except 1.5 mol/l). The resulting solutions were transferred to a Teflon-lined stainless steel autoclave and heated at 200 °C for 1 hour (Figure 1).

It should be noted that the mixtures of FA with CA before the hydrothermal treatment were heterogeneous (opalescence was observed), while those with CitNa were homogeneous. The homogeneity of solutions of a mixture of FA and CitNa is due to the fact that the solubility of FA in a weakly alkaline medium is much higher, than in a weakly acidic medium (solubility in water $4 \cdot 10^{-6}$ mol/l (pH ~ 5.5); solubility at the pH ≥ 6 is $\sim 10^{-3}$ mol/l; data at higher pH values are not available in the literature under study) [16].

The pH of the samples before and after hydrothermal treatment is the same and is shown in Figure 2, *h*. As a result of the hydrothermal treatment of the samples, opalescence disappeared.

1.2. Quantum yield calculation

Calculation of the QY allows one to estimate the efficiency of emission. The relative QY of FNSs was calculated using quinine sulfate in 0.05 mol/l H_2SO_4 as a reference. The QY was calculated with the following equation:

$$\Phi_x = \Phi_{st} \cdot (A_x/A_{st}) \cdot (F_{st}/F_x) \cdot (n/n_0)^2,$$

where Φ is QY, A is absorbance at the excitation

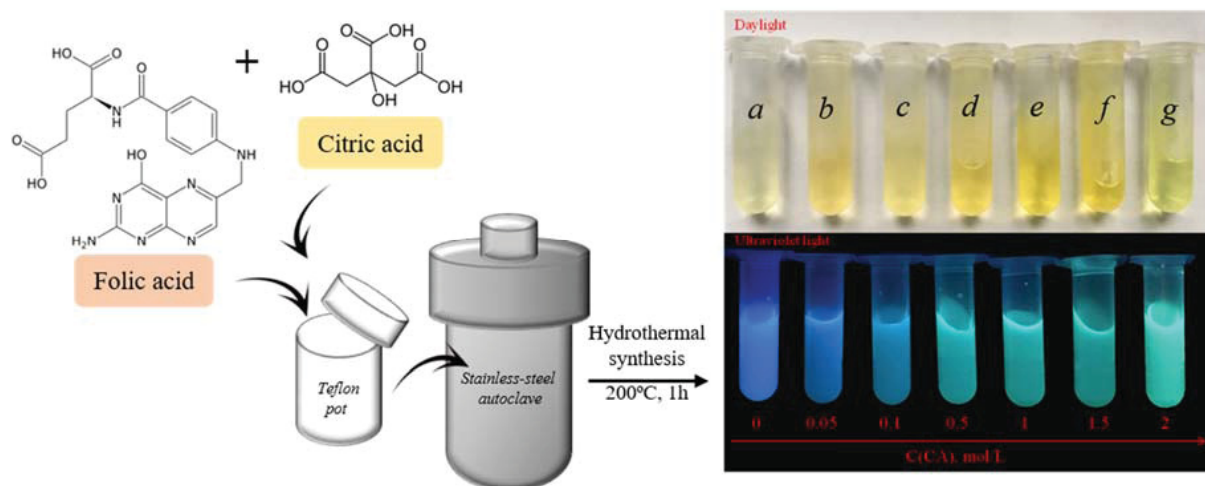


Fig. 1. Scheme of the synthesis of fluorescent nanostructures based on folic and citric acids, and their photographs in daylight and ultraviolet light: *a* – folic acid sample (10^{-3} mol/l) without any additives, *b–g* – samples with citric acid additives 0.05, 0.1, 0.5, 1, 1.5, and 2 mol/l, respectively (colour online)

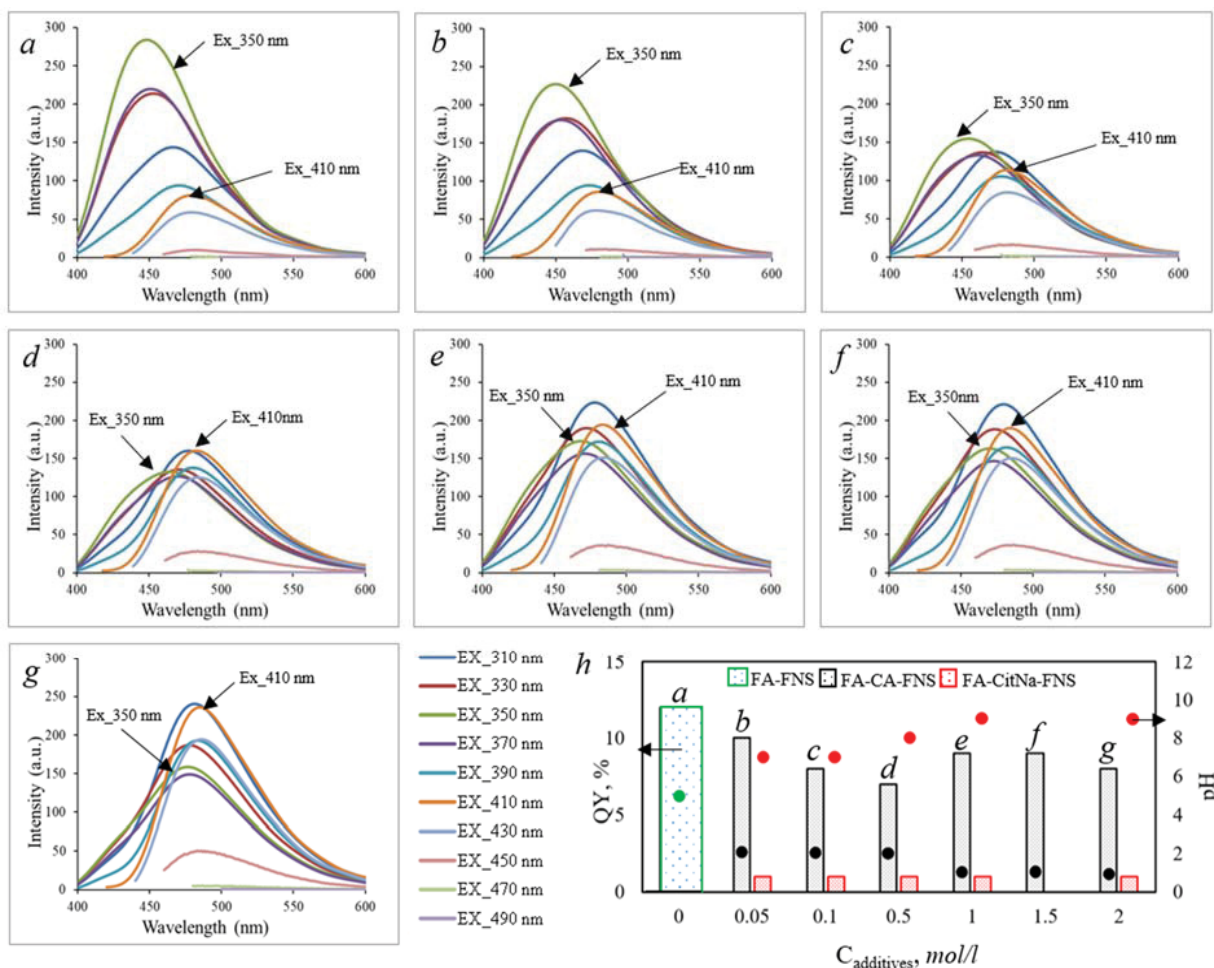


Fig. 2. Fluorescence spectra of the samples obtained at different excitation wavelengths and fixed value of optical density for 350 nm (0.100 ± 0.002) (*a–g*); the values of the quantum yield and of samples obtained on the basis of folic and citric acids, folic acid and sodium citrate (*h*). Additional designations: *a* – folic acid sample (10^{-3} mol/l) without any additives, *b–g* – samples with citric acid additives 0.05, 0.1, 0.5, 1, 1.5, and 2 mol/l, respectively (colour online)



wavelength, F the integrated emission area across the band, and n is the refractive index of the solvent containing the samples (n) and the reference (n_0). The subscript “st” refers to the referenced fluorophore (quinine sulfate in 0.05 mol/l H_2SO_4) with known QY and “x” refers as the samples for the determination of QY. Absorbance of sample and reference were kept 0.100 ± 0.002 at the excitation wavelength of 350 nm.

2. Results and Discussion

The absorption spectrum of FA has several bands; the position and shape of absorption spectra are highly dependent on pH. The pterin fragment of folic acid is responsible for its fluorescent properties and has a characteristic absorption band at 350 nm. In this regard, for the best comparison of the samples, the fluorescence spectra were detected at an optical density (0.100 ± 0.002) at a wavelength 350 nm.

FA in its individual form has fluorescence, the maximum of which is located in the region of 450 nm and is observed at an excitation wavelength of 350 nm, but the QY does not exceed 1%. Since the pterin component of the molecule is responsible for the fluorescent properties of FA, other pterins have similar emission characteristics. This will partially allow us to conclude what contribution the pterin fragment makes to the fluorescent properties of the obtained samples.

As a result of hydrothermal treatment of a colloidal solution of FA (further FA-FNS), its fluorescence increases and the QY increases to 12% (Figure 2, *a*). The maximum fluorescence and the optimal excitation wavelength of FA-FNS coincide with those for FA without any processing.

The samples obtained on the basis of FA and CitNa (further FA-CitNa-FNS) have low fluorescence intensity and high pH (in the range from 7 to 9), the QY does not exceed one percent (Figure 2, *h*). The shape of the spectrum does not change and is similar to that of FA-FNS (Figure 2, *a*). From the data obtained, it can be assumed that CitNa does not lead to the formation of new fluorescent structures, but serves as an alkaline media for FA. This also explains the low values of quantum yields compared to FA-FNS without additives with similar hydrothermal treatment.

The samples obtained on the basis of FA and CA (further FA-CA-FNS) have bright fluorescence in the blue-green region of the spectrum (Figure 1, *b–g*). The fluorescence spectra of samples obtained at various concentrations of CA additives are shown

in Figure 2, *b–g*. The pH of the samples is acidic (in the range from 1 to 2). With an increase in the CA concentration, the shape of the spectrum and the spectral characteristics change significantly, which can be caused by the presence of several fluorescent fractions in the samples, the emission maximum of which is located at 450 and 500 nm. Since the calculation of the quantum yield was carried out by the relative method using quinine sulfate, the fraction with the emission maximum at 450 nm makes the main contribution to the value of the quantum yield, and for the fraction with the emission maximum at 500 nm, the used excitation is less effective. In this regard, the value of the QY of the samples is 7–10% and varies within the determination error. We plan in the future to carry out the determination of the QY according to several standards.

Of greatest interest are the spectra of the samples obtained upon excitation of 350 nm (typical for the pterin fragment of FA) and 410 nm (maximum intensity at the maximum concentration of CA additive). With an increase in the concentration of the CA additive, the ratio of the intensities of fluorescent fractions, the excitation of which occurs at 350 and 410 nm, changes.

At the maximum concentration of CA additive, the maximum fluorescence of FA-CA-FNS is located in a longer wavelength region than of FA-FNS. In this connection, the excitation spectra were recorded at the emission maximums of 450 and 500 nm.

On the excitation spectra of FA-CA-FNS at an emission wavelength of 450 nm (Figure 3, *A*), with an increase in the concentration of the additive, a decrease in the excitation maximum in the region of 350 nm is observed. The fluorescence spectra at this wavelength (Figure 3, *C*) also show a change in fluorescence and a shift of the maximum to the long-wavelength region (Figure 3, *E*).

Excitation spectra of FA-CA-FNS at an emission wavelength of 500 nm for the sample with the lowest additive concentration (0.05 mol/l) exhibit a characteristic maximum for FA at 350 nm (Figure 3, *B, a, b*). However, with a further increase in the concentration of CA, a new band appears in the excitation spectra in the region of 410, the intensity of which increases (Figure 3, *B*). An increase in intensity is also observed in the fluorescence spectra at this wavelength (Figure 3, *D*), the position of the maximum changes insignificantly (Figure 3, *F*).

To exclude the possible formation of FNS based on CA with the same optical properties, we carried out a hydrothermal treatment of CA solution with a concentration of 2 mol/l under similar conditions

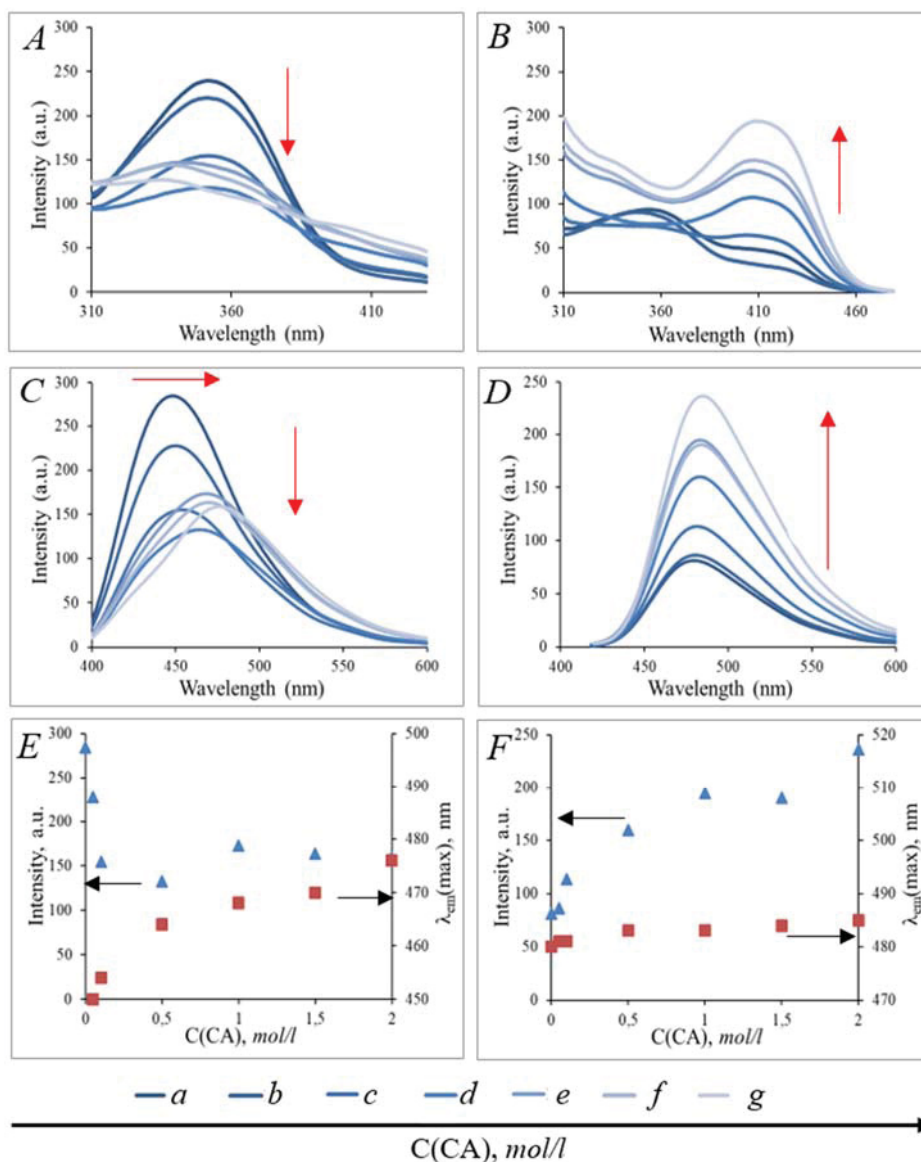


Fig. 3. Excitation spectra obtained at the emission wavelength of 450 and 500 nm, respectively (A, B); fluorescence spectra obtained at excitation lengths of 350 and 410 nm, respectively (C, D); dependence of the intensity at the maximum (blue, triangles) and maximum fluorescence (red, squares) on the concentration of citric acid at excitation lengths of 350 and 410 nm, respectively (E, F). Additional designations for spectra: *a* – folic acid sample (10^{-3} mol/l) without any additives, *b–g* – samples with citric acid additives 0.05, 0.1, 0.5, 1, 1.5 and 2 mol/l, respectively (colour online)

(the concentration of the maximum additive). The resulting structures (future CA-FNS) have a lower intensity than FA-FNS and FA-CA-FNS (quantum yield less than 1%). In this regard, it is not advisable to compare the original fluorescence spectra.

Figure 4 shows the excitation spectra at a maximum emission of 450 nm and fluorescence at an excitation wavelength of 350 nm normalized to unity for the following samples: FA-FNS, CA-FNS and FA-CA-FNS.

Normalized excitation spectra (Figure 4, *a*) demonstrate that excitation in the region of 400 nm is characteristic only for the sample FA-CA-FNS. The location of emission maxima (Figure 4, *b*) allows us to conclude that as a result of hydrothermal treatment of FA and CA, a product with new properties is formed, which also has fluorescent fractions from FA-FNS and CA-FNS.

Thus, the combined hydrothermal treatment of folic and citric acids leads to the formation of new

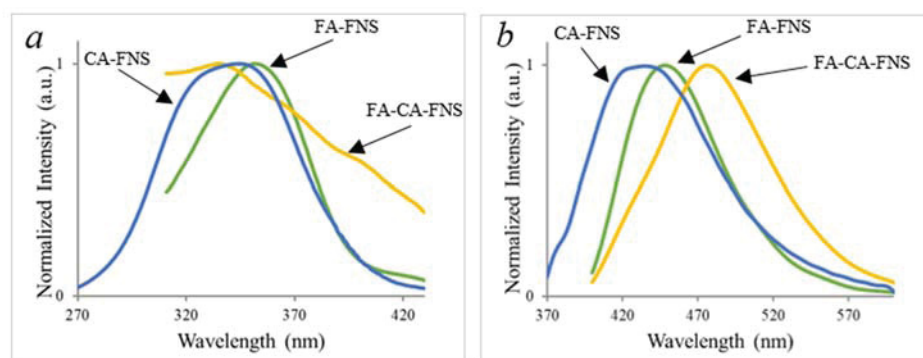


Fig. 4. Excitation spectra obtained at the emission wavelength of 450 (a) and fluorescence spectra obtained at excitation lengths of 350 nm (b) normalized to unity for the following samples: FA-FNS, CA-FNS and FA-CA-FNS (colour online)

fluorescent nanostructures, which consist of several fluorescent fractions with maximum radiation at 450 and 480 nm (optimal excitation 350 and 410 nm, respectively). With an increase in the concentration of citric acid additive, the fluorescence of the first fraction decreases, and the fluorescence of the second fraction increases.

Conclusions

As a result of the work, the effect of citric acid and sodium citrate on the optical properties of fluorescent structures based on folic acid was shown. The combined hydrothermal treatment of folic and citric acids leads to the production of bright fluorescence in the blue-green region of the spectrum with a quantum yield of 7–10%. The fluorescence of the obtained structures is located in a longer wavelength region than that of FA. The presence of FA and bright blue-green fluorescence opens up the possibility of further use of the obtained structures for targeted imaging.

References

- Bhalerao K. D., Lee S. C., Soboyejo W. O., Soboyejo A. B. O. A folic acid-based functionalized surface for biosensor systems. *J. Mater. Sci. Mater. Med.*, 2007, vol. 18, iss. 1, pp. 3–8. <https://doi.org/10.1007/s10856-006-0657-x>
- Chen C., Ke J., Zhou X. E., Yi. W., Brunzelle J. S., Li J., Yong E. L., Xu H. E., Melcher K. Structural basis for molecular recognition of folic acid by folate receptors. *Nature*, 2013, vol. 500, no. 7463, pp. 486–489. <https://doi.org/10.1038/nature12327>
- Zeng L., Luo L., Pan Y., Luo S., Lu G., Wu A. In vivo targeted magnetic resonance imaging and visualized photodynamic therapy in deep-tissue cancers using folic acid-functionalized superparamagnetic-upconversion nanocomposites. *Nanoscale*, 2015, vol. 7, no. 19, pp. 8946–8954. <https://doi.org/10.1039/C5NR01932J>
- Cheng Z., Thorek D. L. J., Tsourkas A. Gadolinium-Conjugated Dendrimer Nanoclusters as a Tumor-Targeted T1 Magnetic Resonance Imaging Contrast Agent. *Angew. Chem.*, 2010, vol. 122, pp. 356–360. <https://doi.org/10.1002/ange.200905133>
- Wang S., Lee R. J., Mathias C. J., Green M. A., Low P. S. Synthesis, Purification, and Tumor Cell Uptake of ⁶⁷Ga-Deferoxamine-Folate, a Potential Radiopharmaceutical for Tumor Imaging. *Bioconjug. Chem.*, 1996, vol. 7, no. 1, pp. 56–62. <https://doi.org/10.1021/bc9500709>
- Lee J. W., Lu J. Y., Low P. S., Fuchs P. L. Synthesis and Evaluation of Taxol-Folic Acid Conjugates as Targeted Antineoplastics. *Bioorg. Med. Chem.*, 2002, vol. 10, pp. 2397–2414. [https://doi.org/10.1016/S0968-0896\(02\)00019-6](https://doi.org/10.1016/S0968-0896(02)00019-6)
- Novikova A. S., Ponomaryova T. S., Goryacheva I. Y. Fluorescent AgInS/ZnS quantum dots microplate and lateral flow immunoassays for folic acid determination in juice samples. *Microchim. Acta*, 2020, vol. 187, pp. 1–9. <https://doi.org/10.1007/s00604-020-04398-1>
- Vostrikova A. M., Kokorina A. A., Mitrophanova A. N., Sindeeva O. A., Sapelkin A. V., Sukhorukov G. B., Goryacheva I. Y. One step hydrothermal functionalization of gold nanoparticles with folic acid. *Colloids and Surfaces B: Biointerfaces*, 2019, vol. 181, pp. 533–538. <https://doi.org/10.1016/j.colsurfb.2019.05.072>
- Thomas A. H., Lorente C., Capparelli A. L., Pokhrel M. R., Braun A. M., Oliveros E. Fluorescence of pterin, 6-formylpterin, 6-carboxypterin and folic acid in aqueous solution: pH effects. *Photochem. Photobiol. Sci.*, 2002, vol. 1, no. 6, pp. 421–426. <https://doi.org/10.1039/B202114E>
- Tsyupka D. V., Mordovina E. A., Sindeeva O. A., Sapelkin A. V., Sukhorukov G. B., Goryacheva I. Y. High-fluorescent product of folic acid photodegradation: Optical properties and cell effect. *J. Photochem. Photobiol. A*, 2021, vol. 407, pp. 113045. <https://doi.org/10.1016/j.jphotochem.2020.113045>
- Vora A., Riga A., Dollimore D., Kenneth A. S. Thermal stability of folic acid. *Thermochim. Acta*, 2002, vol. 392–393, pp. 209–220. [https://doi.org/10.1016/S0040-6031\(02\)00103-X](https://doi.org/10.1016/S0040-6031(02)00103-X)



12. Campos B. B., María Moreno Oliva, Rafael Contreras-Cáceres, Enrique Rodríguez-Castellón, José Jiménez-Jiménez, Joaquim C. G. Esteves da Silva, Manuel Algarra. Carbon dots on based folic acid coated with PAMAM dendrimer as platform for Pt (IV) detection. *Journal of Colloid and Interface Science*, 2016, vol. 465, pp. 165–173. <https://doi.org/10.1016/j.jcis.2015.11.059>
13. Zhu S., Zhao X., Song Y., Lu S., Yang B. Beyond bottom-up carbon nanodots: Citric-acid derived organic molecules. *Nano Today*, 2016, vol. 11, no. 2, pp. 128–132. <https://doi.org/10.1016/j.nantod.2015.09.002>
14. Kokorina A. A., Prikhozhdenko E. S., Sukhorukov G. B., Sapelkin A. V., Goryacheva I. Yu. Luminescent carbon nanoparticles: Synthesis, methods of investigation, applications. *Russ. Chem. Rev.*, 2017, vol. 86, no. 11, pp. 1157–1171 (in Russian). <https://doi.org/10.1070/RCR4751>
15. Kokorina A. A., Ermakov A. V., Abramova A. M., Goryacheva I. Yu., Sukhorukov G. B. Carbon nanoparticles and materials on their basis. *Colloids Interfaces*, 2020, vol. 4, no. 4, pp. 42. <https://doi.org/10.3390/colloids4040042>
16. Wu Z., Hou C., Qian Y. Solubility of Folic Acid in Water at pH Values between 0 and 7 at Temperatures (298.15, 303.15, and 313.15) K. *J. Chem. Eng. Data*, 2010, vol. 55, no. 9, pp. 3958–3961. <https://doi.org/10.1021/jc1000268>

Поступила в редакцию 18.02.2021, после рецензирования 12.04.2021, принята к публикации 04.05.2021

Received 18.02.2021, revised 12.04.2021, accepted 04.05.2021